Low-temperature radiant cooling panel for hot and humid climate

Gongsheng Huang[a], Nan Zhang[b], Yuying Liang[c]

[a] Department of Architecture and Civil Engineering, City University of Hong Kong, Kowloon, Hong Kong, email: gongsheng.huang@cityu.edu.hk

[b] Department of Architecture and Civil Engineering, City University of Hong Kong, Kowloon, Hong Kong, email: nzhang88-c@my.cityu.edu.hk

[c] Department of Architecture and Civil Engineering, City University of Hong Kong, Kowloon, Hong Kong, email: Yuying.Liang@my.cityu.edu.hk

Abstract. In this paper, the heat transfer and thermal environment of air-layer integrated radiant cooling panel (AiCRCP) was studied experimentally. AiCRCP was proposed in 1963, which was characterized by the use of an infrared-radiation transparent (IRT) membrane to separate the panel's radiant cooling surface from its external air-contact surface. Therefore, the panel's radiant cooling surface temperature can be reduced to increase the cooling capacity, while its external air-contact surface, due to the thermal resistance provided by the air layer and the IRT membrane, can be easily maintained at a high temperature to reduce condensation risks. The thermal performance of AiCRCP was investigated using a prototype. Several scenarios were tested to analyze the thermal performance of prototype, and the cooling capacity of the AiCRCP was also investigated according to the thermal performance of the prototype. The results demonstrated that this new type of radiant cooling systems could be more preferable to be implemented in hot and humid climates.

Keywords. Radiant cooling, air-layer integrated ceiling radiant cooling panel, IRT membrane, condensation, cooling capacity
DOI: https://doi.org/10.34641/clima.2022.395

1. Introduction

Radiant cooling has many benefits, such as its high thermal comfort, lower energy use, quiet operation, and smaller equipment footprint, compared with the methods of cooling air of indoor spaces through air circulation [1-2]. However, radiant cooling applications face great challenges in hot and humid climates from condensation and their limited cooling capacity [3]. In its cooling mechanisms, whether through panel cooling or slab cooling [4], the radiant surface is also the air-contact surface, as shown in Fig. (1a), where a conventional ceiling radiant-cooling panel (CRCP) is used. In this CRCP, the cooling capacity increases with the decrease of the radiant-cooling surface temperature, but this will increase the risk of condensation. This dilemma has inhibited the commercialization of radiant cooling in hot and humid climates [5], and explains why CRCPs should be used together with other air-cooling systems in practical applications to provide enough cooling for thermal comfort [6].

Many attempts have therefore been made to solve the condensation problem while increasing the cooling capacity [7, 8]. A typical method is to maintain a low relative humidity so low radiant temperature can be used [9, 10], but this dehumidification is costly and risks degrading the thermal comfort. By realizing that the radiant surface must be isolated from the air-contact surface to essentially solving this dilemma, Morse proposed a radiant-cooling panel covered with a sheet spaced several centimeters from it, filled with dry air, and sealed to prevent room air from contacting the cold radiant-cooling surface [11], referred to as an *air-layer-integrated radiant-cooing panel* (AiCRCP) and illustrated in Fig. (1b). Thus, the air-contact surface and radiant cooling surface in the AiCRCP are physically separated.

It should be noted that the cover sheet must be transparent to the energy radiated from a body at a temperature range of 29.4°C to 35°C, and thus titled as infrared transparent (IRT) membrane. It enables the panel to act as a radiation heat sink, and heat from occupants in the vicinity can radiate through the transparent cover to the cold plate behind. Teitelbaum et al. [12] revisited this design, investigating several manufactured materials, such as low/high density polyethylene and polypropylene, using Fourier transform infrared

(FTIR) spectroscopy to analyze its thermal performance. They also investigated the panel depth (spacing between the radiant-cooling panel and the membrane) to balance radiation, conduction, and convection when AiRCPs was applied to an outdoor environment.

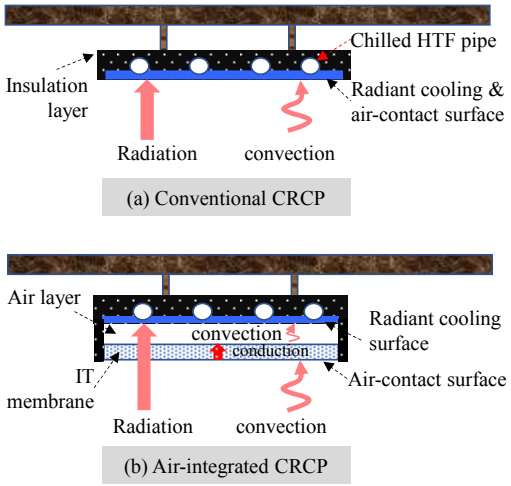

Fig 1. - Diagrams of (a) the conventional radiant cooling unit, (b) the air-integrated CRCP.

Teitelbaum et al.'s work motivated the studies on AiRCPs and AiCRCPs (here AiCRCP is used as the panel is installed on the ceiling for indoor cooling). Most of these studies, similar to Teitelbaum et al.'s work [12, 13], were focused on the thermal performance created by AiCRCPs. For example, Xing et al. [14] studied the influence of several factors, such as the flow regimes inside the air-layer, infrared transmissivity/emissivity of the IR-transparent membrane and relative humidity of indoor air, on the thermal performance of AiCRCPs. Sheppard [15] developed a heat balance model for AiRCPs to estimate their operational membrane temperature and cooling capacity. while Du et al. alalyzed the thermal performance of an AiCRCP with double-skin infrared-transparent membranes [16].

In our research group, Zhang et al. established a two-flux heat transfer model for the AiCRCP, to analyze the optical, physical and thermal properties of the IR-transparent membrane [17]. Liang et al. investigated the thermal environment and thermal comfort created by an AiCRCP with different low radiant temperatures (−2.3°C to 15°C) in a small thermal chamber using computational fluid dynamics simulations, and they demonstrated that both local and general thermal comfort indices, defined by ASHARE standards, could be satisfied even when the AiCRCP operated at a very low radiant temperature (e.g. −2.3°C) [18].

Previous literature has demonstrated that the enhanced cooling capacity and reduced condensation risk of AiCRCPs in addition to the thermal comfort they can maintain give them potential applications in hot and humid climates. However, most of the work reviewed above was based on simulation or numerical studies. In this paper, the cooling performance of an AiCRCP prototype and the thermal environment created by the AiCRCP were investigated using experiments, which showed that the AiCRCP could provide higher cooling capacity and better condensation prevetion.

2. Theoretical background

The heat transfer process of the AiCRCP is shown in Fig. 1(b), where the heat exchange between the AiCRCP and its thermal environment is mainly through two mechanims. One is radiation that occurs directly between the AiCRCP and its thermal environment; and other is the combination of convenction and conduction.

In the first mechanism, since the IRT membrane is assumed to have a poor ability to absorb infrared radiative heat flux and the air-layer is transparent to infrared radition, the radiative cooling power of the radiant cooling surface will not be much affected by the IRT membrane.

In the second mechanism, heat is firstly transfered to the IRT membrane from the air surrounding the AiCRCP through convection, and to the raidant cooling surface through the dyr air convenction (major) and conduction (minor). It should be noted that the IRT membreme is thin, its internal surface and exteral surface temperature could be consider as the same in the analysis of the thermal performance of AiCRCP.

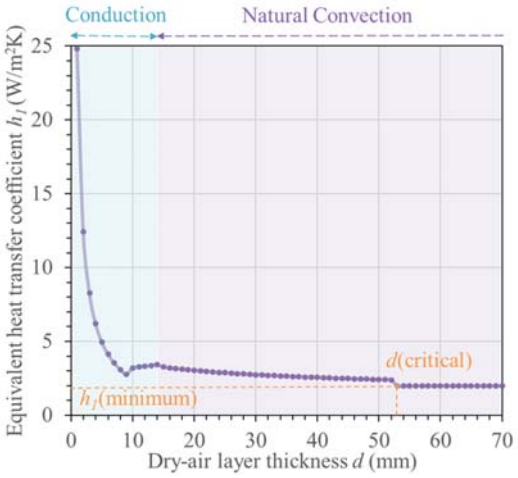

Fig. 2 - The heat transfer coefficient of an enclosed air layer [17].

Because the air layer has a large thermal resistance to both convection and conduction, as shown in Fig 2. [17], the IRT membrane can be maintained at a high temperature even if the radiant cooling temperature is low, for example 5°C (much lower than 17°C used in conventional CRCPs). Therefore, a low radiant cooling temperature can be used to

enhance the cooling capacity of the AiCRCP without increasing the condensation risk.

3. Experiment setup

3.1 Prototype of AiCRCP

Currently there is one prototype of AiCRCP in our laboratory with the dimension of 1 m × 1 m. This prototype uses a piece of aluminum plate: on one side high emissivity paint ($\varepsilon \approx 0.95$) was coated and used as cooling radiant surface, and on another side heat transfer fluid (HTF) pipes were attached and fixed using screws. The layout of the HTF pipes is shown in Fig. 3 (a). Thermal paste (grease) was used to increase the thermal conductivity between the HTF pipe and the aluminum plate, shown in the photo of Fig. 3 (b). This side was covered with a insulation layer (Nitrile rubber) to prevent cooling loss. A 20 μm thick low density *Polyethylene* (LDPE) was used as the IR-transparent membrane to seal a dry-air layer to separate the air-contact and radiant-cooling surfaces. A photo of the prototype is given in Fig. 3 (c). The prototype was connected with an air-cooled chiller that can provide heat transfer fluid with the temperature from −10°C to 20°C with the rated cooling capacity of 5.67 kW and coefficient of performance (COP) of 3.86. The membrane has a good IR transparency property as shown in Fig 3. (d), where the spectral transmittance was measured using FTIR (Spectrum Two, PerkinElmer).

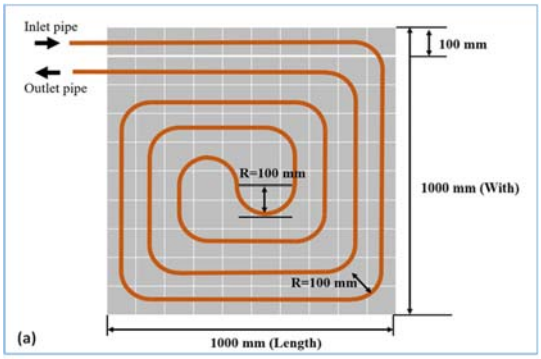

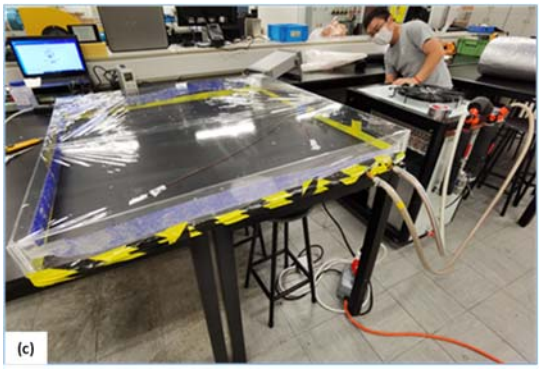

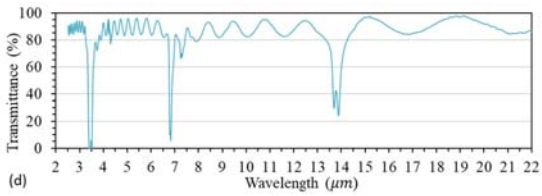

Fig. 3 - (a) HTF pipe layout on the radiant cooling panel; (b) The radiant cooling panel covered by an insulation layer; (c) LDPE membrane covering the panel and sealing a dry air layer; (d) IR spectral transmittance through LDPE membrane using FTIR.

3.2 Thermal chamber

The available thermal chamber is made of a wood layer, a metal layer, a thin insulation layer and an inner finish layer of mineral fiber. It is placed on a movable structure as shown in the photo of Fig. 4 (a). Fig. 4 (b) shows the internal view of the chamber. There is small window on the back with the dimension of 1.2 m×0.5 m.

A number of sensors/flow meters were installed to measure the temperature, flow and humidity. The measured qualities, number of sensors and sensor uncertainty were summarized in Table 1. Note that an FLIR infrared camera was also used to measure the radiant cooling surface temperature. All the measured data were collected using a data logger (SWEMA), connected to a computer for data analysis.

Tab. 1 - Measured quantities, number and uncertainty of sensors.

Measured Quantity	Sensor	Number	Uncertainty
HTF Fluid temperature	T-type Thermocouple	2	±0.5°C
Surface temperature	T-type Thermocouple	18	±0.5°C
Dry bulb air temperature	Swema 03+	1	±0.1°C
Indoor air velocity		1	±0.04m/s
Relative humidity	Swema HC2A-S	1	±0.8%RH
Globe temperatur	Swema 05	1	±0.1°C

e HTF flow rate	Turbine pulse flowmeter	2	±0.5%
Infrared temperature	FLIR infrared camera	1	±2%

Fig. 4 – (a) an external view of the thermal chamber and (b) an internal view of the chamber.

4. Experimental results and analysis

4.1 Testing scenarios

During the experiment, the thermal chamber was moved into a conditioned large hall, where the space temperature and humidity was maintained to be relatively stable in order to reduce the influence of the environmental disturbance from external weather conditions. Inside the thermal chamber, the cooling panel was installed horizontally on the ceiling, facing downward and working as ceiling cooling. In the test, the controlled variables were the indoor air temperature inside the thermal chamber and the radiant cooling temperature of the AiCRCP. The indoor air temperature was adjusted by several small heaters; the humidity was adjusted by a humidifier; while the radiant cooling temperature was controlled by the air-cooled chiller.

There were three testing scenarios, defined according to the total power of the heaters and listed in **Tab 2**. In scenario 1, the total power of the heater was the highest; while it was the lowest in scenario 2. In each scenario, the HTF supply temperature was varied in the range of -5~15℃, and the cooling panel radiant surface temperature had a gradient change between 1℃ and 19℃. The RH of the indoor air temperature was controlled at 3 levels, i.e. 70%, 60% and 50%. When any variable was changed, the temperatures were measured 20 min after stability. No mechanical ventilation was used during the experiment.

Tab. 2 – Scenarios designed for the experiment.

Scenario	Total power of the heaters (W)	Cooling panel temperature (℃)
1	450 (RH=70%, 60%, 50%)	1~19
2	210 (RH=70%, 60%, 50%)	
3	0 (RH=70%, 60%, 50%)	

4.2 Temperature of the IRT membrane

Since the temperature of the IRT membrane surface (toward indoor air side) is an important variable that indicates the capability of the AiCRCP for condensation prevention, it was analysed at the beginning. Please note that it is required at least 1°C higher than the dew point of indoor air to avoid condensation risk [2].

Fig. 5 shows the average temperature of the IRT membrane under different radiant cooling panel temperature and different indoor air temperature and humidity. The dash lines are the dew point temperature of the indoor air. It can be seen that the dew point temperature decreased with the decrease of the cooling radiant temperature when the relative humidity was a constant. When the membrane temperature was equivalent to the dew point temperature, the cooling panel temperature was marked with a red circle in Fig. 5.

As shown in Fig. 5 (a) where RH was maintained at 70%, the cooling panel temperature should be higher than 13.5°C, 8.5□ and 3□ when the indoor air temperature was 28.9°C, 25□ and 19.4°C, respectively. However, when RH=60%, the cooling panel temperature should be higher than 6°C when the environmental temperature was 29°C. When the indoor air was lower than 25°C, the condensation would not occur on the membrane even if the cooling surface temperature was reduced to below 2°C. When RH=50%, the results in Fig. 5 (c) showed that no condensation occurred on the membrane in these three different indoor air temperatures even the cooling panel temperature was reduced to 1°C.

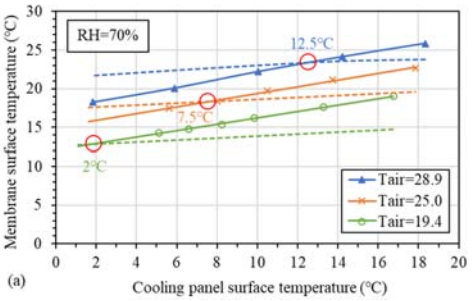

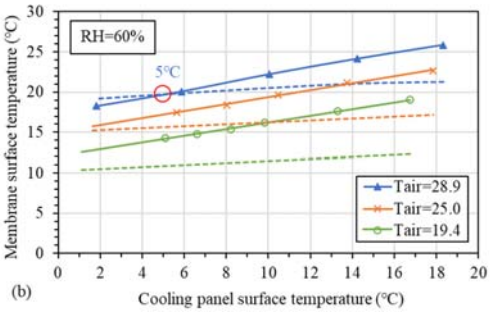

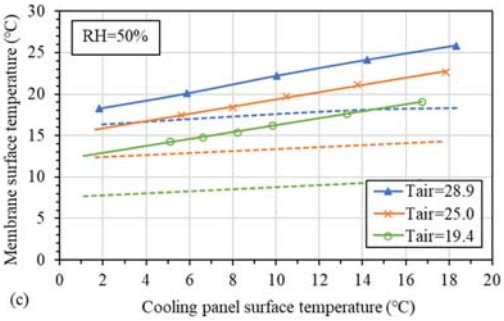

Fig. 5 – IRT membrane temperature in different indoor environments (a) RH = 70%, (b) RH = 60%, and (c) RH = 50%.

To further analyse the capability of the condensation prevention of the AiCRCP, the minimum allowable cooling panel temperature allowed was defined, which was the minimal temperature of the panel that can guarantee the IRT membrane temperature being 1°C higher than the dew point of the indoor air. The differences between the minimum allowable cooling panel temperature of the AiCRCP and the conventional ceiling radiant cooling panel were shown in Fig. 6 when RH=70% and RH=60%. The differences of the minimum cooling panel temperature was relatively constant when RH was same. For example, when RH=70% the minimum allowable temperature of the AiCRCP was around 10.8 lower than the conventional CRCP; and when RH=60%, the value was about 15°C. Therefore, the AiCRCP has a good performance in preventing condensation in hot and humid climates with lower radiant temperature.

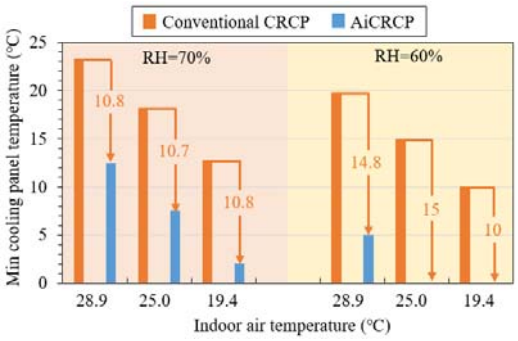

Fig. 6 – The minimum allowable cooling panel temperature of the AiCRCP and the conventional CRCP.

5. Cooling capacity of the AiCRCP

The cooling capacity of an AiCRCP depends on the thermal environment that is conditioned by the AiCRCP. Here we considered a room with the dimensions of 4 m× 4m ×3m. We assumed that the whole ceiling was used as AiCRCP. The walls and floors had the emissivity of 0.9. Referring to the Fig. (2d), the IRT transmittance of the membrane was assumed to be 80%. The temperature of the room air and the wall/floor surfaces were assumed to be 26°C.

The radiative heat transfer was calculated by Eqn. (1), where τ is the transmittance of the IRT membrane and Q'_{rad} is the radiation between surface 1 and 2 without membrane. In the calculation, view factors were considered and the equation matrix of all surfaces in the indoor environment was shown as Eq. (2), where ε is the emissivity, σ is the Boltzmann constant, J is the effective radiation, and $X_{i,j}$ is the view factor from surface i to j. The radiation heat flux between the cooling panel and other surfaces was calculated by Eq. (3), assuming the cooling panel being surface 1.

$$Q_{rad} = \tau \cdot Q'_{rad} \tag{1}$$

$$\left.\begin{array}{l} J_1\left(X_{1,1} - \frac{1}{1-\varepsilon_1}\right) + J_2X_{1,2} + J_3X_{1,3} + \cdots + J_nX_{1,n} = \frac{\varepsilon_1}{\varepsilon_1 - 1}\sigma T_1^4 \\ J_1X_{2,1} + J_2\left(X_{2,2} - \frac{1}{1-\varepsilon_2}\right) + J_3X_{2,3} + \cdots + J_nX_{2,n} = \frac{\varepsilon_2}{\varepsilon_2 - 1}\sigma T_2^4 \\ \cdots\ \cdots \\ J_1X_{n,1} + J_2X_{n,2} + \cdots + J_n(X_{n,n} - \frac{1}{1-\varepsilon_n}) = \frac{\varepsilon_n}{\varepsilon_n - 1}\sigma T_n^4 \end{array}\right\} \tag{2}$$

$$Q_{rad} = \tau \cdot \frac{\varepsilon_1}{1-\varepsilon_1} \cdot (\sigma T_1^4 - J_1) \tag{3}$$

The convective heat transfer was calculated according to the conservation of energy as shown in Eq. (4), where h_c and h_a were the heat transfer coefficients in the sealed air gap and room air side, T_c was the cooling panel temperature, T_m was the membrane temperautre and T_a was the indoor air temperature. Eq. (4) indicated that the heat transfer between the radiative cooling surface and

the IRT membrane should be equivalent to the amount between the IRT membrane and the room air.

$$Q_{conv} = h_c \cdot (T_m - T_c) = h_a \cdot (T_a - T_m) \quad (4)$$

In Eq. (4), the heat transfer coefficient h_c of the sealed air gap was calculated from Eqn. (5), where Gr is Grashof number, Pr is Prandtl number, λ is the thermal conductivity of dry air and d is the thickness of the air gap. Noted that Eq. (5) was also used to generate Fig. (2). Using the measurements of T_m, T_c and T_a in the experiments that were discussed in Section 4, h_a was approximated using a data fitting method.

$$h_c = \begin{cases} 0.059\frac{\lambda}{d}(Gr \cdot Pr)^{0.4}, 1700 < Gr \cdot Pr < 7000 \\ 0.212\frac{\lambda}{d}(Gr \cdot Pr)^{1/4}, 7000 < Gr \cdot Pr < 3.2 \cdot 10^5 \\ 0.061\frac{\lambda}{d}(Gr \cdot Pr)^{1/3}, Gr \cdot Pr > 3.2 \cdot 10^5 \end{cases} \quad (5)$$

The cooling capacity was the sum of radiative and convective heat fluxes. The cooling capacity of the AiCRCP was compared with that of the conventional CRCP in Fig. 7. When the RH was 70%, 60%, and 50%, the dew point temperatures of the room air were 20.12°C, 17.66°C and 14.81°C, respectively. Therefore, the cooling panel temperature of the conventional CRCP were set as 21°C, 19 °C and 16°C (approximated 1°C above the dew point). To maintain the IRT membrane temperature at 21°C, 19 °C and 16°C, the minimum allowable cooling panel temperatures of the AiCRCP were 13°C, 8°C and 2 °C respectively.

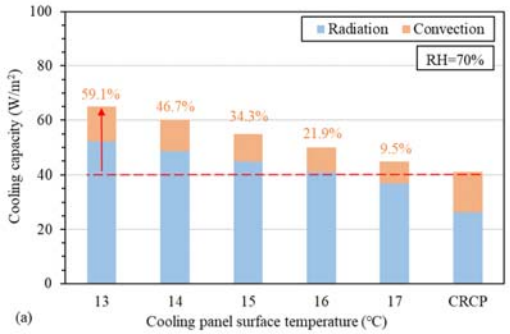

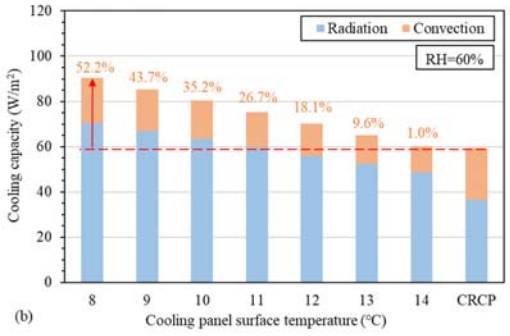

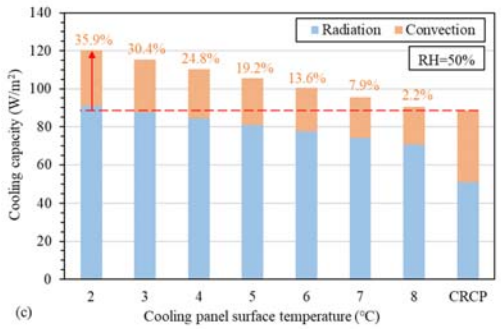

Fig. 7 – The cooling capacity of the AiCRCP and conventional CRCP.

Fig. 7 (a) showed the comparison when RH was 70%. The cooling capacity of the conventional CRCP was 40 W/m² using a radiant temperature of 21°C. 7.5% cooling capacity enhancement was achieved by the AiCRCP when its radiant cooling temperature was 17°C. Since the minimum allowable cooling panel temperature of the AiCRCP could be down to 13°C, the maximum cooling capacity of AiCRCP reached 63.63 W/m², improved by 59.1%.

Fig. 7 (b) showed the comparison when RH was 60%. At this condition, the cooling capacity of the conventional CRCP was 59 W/m² using a radiant temperature of 19°C. Similar cooling capacity was achieved by the AiCRCP when its radiant cooling temperature was 14°C. Since the minimum allowable cooling panel temperature of the AiCRCP could be down to 8°C, the maximum cooling capacity of AiCRCP was improved by 52.2%, reaching 90 W/m².

The comparison when RH was 50% was shown in Fig. 7 (c), where the cooling capacity of the conventional CRCP was 89 W/m² using a radiant temperature of 16°C. When the radiant cooling temperature of the AiCRCP was 8°C, 2.2% cooling capacity improvement was achieved. Similarly, when we considered the minimum allowable cooling panel temperature of the AiCRCP that could be down to 2°C, the maximum cooling capacity of AiCRCP reached 121 W/m², improved by 35.9%.

Fig. 7 also showed that due to a higher air contact surface temperature and a lower radiant surface temperature, the radiative heat flux of the AiCRCP was increased, while the convective flux was decreased when compared to the conventional CRCP. The radiative heat flux to the convective could be as high as 3.5:1. In the conventional CRCP, the ratio was typically 1.3 ~ 1. The enhanced radiative heat flux will benefit the heat exchange directly between heating sources (such as occupants) and the cooling panel.

6. Concluding remarks

This paper investigated the thermal performance of

a prototype of AiCRCP experimentally and then analysed its cooling capacity of AiCRCP in a simple room environment based on the thermal performance of the AiCRCP prototype. The results have shown that

- The AiCRCP has much enhanced capacity to prevent condensation even in hot and humid climates. Due to a large thermal resistance from the sealed air layer, the IRT membrane can be maintained at a high temperature even when the radiant temperature is controlled to a very low temperature.

- Due the possibility of using a low temperature, the cooling capacity of the AiCRCP can be enhanced significantly. At a higher humid environment, for example RH = 70%, the cooling capacity can be improved around 60%.

Thus, the thermal performance of the AiCRCP could make it more preferable when the technique of ceiling radiant cooling is adopted in hot and humid climates.

7. Acknowledgement

The research work presented in this paper was supported by a grant from the Research Grants Council of the Hong Kong Special Administrative Region, China (Project No. 11212919).

8. References

[1] Kim K.W., Olesen B.W., Radiant heating and cooling systems: Part 2, *ASHARE Journal* 2015; 57: 28-37.

[2] Rhee K.N., Kim K.W., A 50 year review of basic and applied research in radiant heating and cooling systems for the built environment, *Building and Environment* 2015; 91: 166-190.

[3] Mumma S.A., Ceiling panel cooling systems, ASHRAE Journal 2001; 43: 28-32.

[4] Rhee K.N., Olesen B.W., Kim K.W., Ten questions about radiant heating and cooling systems, *Building and Environment* 2017; 112: 367-381.

[5] Zhang L.Z., Niu J.L., Indoor humidity behaviors associated with decoupled cooling in hot and humid climates, *Building and Environment* 2003; 38: 99-107.

[6] Shin M.S., Rhee K.N., Park S.H., Yeo M.S., Kim K.W., Enhance of cooling capacity through open-type installation of cooling radiant ceiling panel systems, Building and Environment 2019; 148: 417-432.

[7] Ning B., Chen Y.M., Liu H., Zhang S., Cooling capacity improvement for a radiant ceiling panel with uniform surface temperature distribution, *Building and Environment* 2016; 102: 64-72.

[8] Zhong Z.W., Jiu J.L., Ma W., et al., An experimental study of condensation on an aluminum radiant ceiling panel surface with superhydrophobic treatment, *Energy and Buildings* 2021; 252: 111393.

[9] Hao X., Zhang G., Chen Y., Zou S., Moschandreas D.J., A combined system of chilled ceiling, displacement ventilation and desiccant dehumidification, *Building and Environment* 2007; 42: 3298-3308.

[10] Binghooth A.S., Zainal Z.A., Performance of desiccant dehumidification with hydronic radiant cooling system in hot humid climates, *Energy and Buildings* 2012; 51: 1-5.

[11] Morse R., Radiant cooling. *Architect. Sci. Rev.* 1963; 6: 50–53.

[12] Teitelbaum E., *et al.*, Revisiting radiant cooling: Condensation-free heat rejection using infrared-transparent enclosures of chilled panels. *Architect. Sci. Rev.* 2019; 62: 152–159.

[13] Teitelbauma E., Chen K.W., Dorit Aviv D. , et al., Membrane-assisted radiant cooling for expanding thermal comfort zones globally without air conditioning, *PNAS* 2020; 117: 21162–21169.

[14] Xing D.M, Li N.P., Cui H.J., Zhou L.X., Liu Q.Q., Theoretical study of infrared transparent cover preventing condensation on indoor radiant cooling surfaces, *Energy* 2020; 201: 117694.

[15] Sheppard D., Integrating membrane-assisted radiant cooling panels in building energy simulation, Master thesis, The University of British Columbia, Canada, December 2020.

[16] Du K., Wu H.J., Huang G.S., Xu X.H., Liu Y.C., Condensation-free radiant cooling with double-skin infrared-transparent membranes, *Building and Environment* 2021; 193: 107660.

[17] Zhang N., Liang Y., Wu H., Xu X., Du K., Shao Z., Zhou X., Huang G.S., Heat transfer modelling and analysis of air-layer integrated radiant cooling unit, *Applied Thermal Engineering*, 2021; 194: 117086.

[18] Liang Y.Y., Zhang N., Wu H.J., Xu X.H., Du K., Yang J.M., Sun Q., Dong K.J., Huang G.S., Investigation on the thermal comfort of the environment built by decoupled radiant cooling units with low radiant cooling temperatures, *Building and Environment* 2021;

206: 108342.

Data Statement

d. Data sharing not applicable to this article as no data sets were generated or analysed during the current study.